JOURNAL OF MULTIFUNCTIONAL MATERIALS & PHOTOSCIENCE
8(1), June 2017, pp. 21-38

Review of Material Design various Graphene based Semiconductors Photocatalysis for CO_2 Reduction

Asghar Ali, Won-Chun Oh *

Department of Advanced Materials Science & Engineering, Hanseo University, Seosan 31962, Korea

Abstract: In recent times, immoderate consumption of fossil fuel and depletion of existing resources is concentrate the research and development of substitute future energy options that can directly diminish and process ever-increasing carbon dioxide (CO_2) emissions. Since CO_2 is a thermodynamically stable compound, its reduction must not dissipate additional energy or increase net CO_2 emissions. Renewable sources like solar energy provide freely available and continuous light supply required for driving this conversion process. Hence, the use of solar energy to drive CO_2 photocatalytic reactions concurrently addresses the above mention challenges, while producing feasible fuels or chemicals applicable for use in existing energy framework. Recent progress in this area has focused on the development (fabricate and design) of new materials for CO_2 reduction purification technologies to keep the environment safe and secure. Moreover also highlight various CO_2 reduction/purification catalyst materials used in recent advanced technologies.

Keywords: CO_2 Photoreduction, Photocatalysis, Graphene, UV/Vis Light, Artificial photosynthesis

1. Introduction

Recently, the expanding CO_2 concentration in the air due to the continually developing utilization of non-renewable energy sources has caused inconvenient ecological contamination [1-5]. Yearly CO_2 emission relentlessly expanded in recent years due to the vast consumption of the fossil fuels. Since the gathering of CO_2 can trap heat in the air, it is not astound that the average worldwide surface temperature on this planet simultaneously increased with the CO_2 emission in recent years [6-8]. Consequently, searching for sustainable and environmentally friendly energy resources has turned out to be an urgent task for the long-term development of human society [9-15]. It is assessed that the CO_2 focus in the air rises each year at a rate higher than 2% and subsequently, the normal temperature on the Earth's surface has expanded around 0.4–0.8 æ%C over the last century. It is anticipated that the worldwide temperature may ascend by 1.9 æ%C and that the level of CO_2 may move to 590 ppm. A worldwide temperature alteration

*Corresponding author: *wc_oh@hanseo.ac.kr*

causes the dissolving of the ice at the poles, the expansion of the seas and the loss of expansive ice amounts from Greenland and Antarctica which cause an increment of the ocean level. The extraordinary meteorological wonders (strange winds, aridity, floods) constitute some additional results of the Greenhouse impact. For instance, a reduction in precipitation in certain area may decrease the required water supplies for peoples, biological systems, and agriculture. The improved precipitation in different regions constitutes an additional troubling factor. Furthermore, the most recent 25 years the expansion in CO_2 concentration is remarkable and may prompt a conceivable change of the radiative balance on the planet. Besides, CO_2 positively is an essential gas in the environment because its takes parts in the Carbon cycle as a carbon source [16-19]. So as to accomplish the lessening in the CO_2 concentration in the environment, the carbon dioxide neutral cycle, ought to be completed. A few factors are essential for the continuation of this cycle, for example, the recycling of CO_2 after the fuel's ignition, the utilization of renewable energy (wind energy, solar energy and so on) [20].In this regard, one almost infinite natural energy resource is sunlight reaching the Earth's crust [21]. Since the solar energy is considered as one of the boundless and environmentally green energy sources, much consideration has been paid to the change of approaching sunlight based energy into important valuable solar fuels[22-27]. Among different potential outcomes, photocatalytic CO_2 reduction into solar fuels such as, CH_4, HCO_2H, CH_2O, and CH_3OH has been known as a standout amongst the most encouraging innovations since it can simultaneously produce useful solar fuels and impersonate the CO_2 concentration in the atmosphere[28-33]. Inoue et al. reported that the photo-reduction of CO_2 with H_2O can result in several products including HCOOH, HCHO, CH_3OH, and CH_4 [34]. However, proper attention is needed to design and develop efficient photocatalytic systems to reduce CO_2 and convert it into useful products [35-37]. Several semiconductor photocatalysts have been used to reduce CO_2. For example, titanium dioxide (TiO_2) has been considered as one of the most favorable photocatalysts due to its chemical stability, non-toxicity, low cost, and superior activity [10, 38, 39]. TiO_2 has several crystal phases in addition to an amorphous phase. However, for photocatalysis, it has been observed that anatase is the most dynamic form of TiO_2. The presence of defects in the crystal structure is unfavorable for the photocatalytic activity, due to defects; amorphous titania is always considerably much less photocatalytic efficiency. When prepared by sol–gel at normal temperatures, amorphous titania is the first material achieved, but raising temperature below 350 C increases significantly the crystallinity of the solid towards the thermodynamically more stable anatase phase. This phase transition results in a considerable increase in photocatalytic activity. And further increasing temperature (greater than 350 C) converts anatase into rutile. Although rutile is also a semiconductor and has somewhat smaller bandgap with an absorption tail into the visible region, the photocatalytic activity of this titania crystal phase is generally lower than that of anatase. And much higher temperatures result in the formation of brookite that is totally inactive from the photocatalytically point of view. Therefore many investigate endeavors have been performed in understanding the fundamental process and in improving the photocatalytic effieciency of TiO_2. Such studies are frequently related to energy renewal and energy storage. Application to

environmental cleanup has been one of the most convenient ways on photo catalysis[40]. However, the photocatalytic efficiency of TiO_2 is limited by its band gap and rapid charge carrier recombination dynamics [39, 41]. Therefore, some modifications can be carried out to improve the efficiency of TiO_2, such as doping TiO_2 with metals [42, 43] or nonmetals [44, 45] and coupling TiO_2 with narrow band gap semiconductors [46, 47]. Graphene, a carbon nanomaterial [36].

2. Graphene

Graphene, basically single layer carbon 2D nanosheet with hexagonal packed lattice structure material, occurring in graphite intercalation compound. In the initial step these intercalated layers has been isolated through synthetic oxidation amid the compound combination. Graphene, basically characterize as a disconnected single layer of carbon hexagon consist of sp^2 hybridized C-C holding with conjugated ð electron cloud. The graphene'' initially proposed by in 1986 as a separated single 2D sheet of carbon atom has gotten awesome arrangement of consideration in logical and building fields since its leap forward disclosure by Geim and Novoselov in 2004[48-52]. Graphene has promising candidate for photo catalytic CO_2 reduction due to their unique properties, such as large surface area, good conductivity, and high flexibility[53, 54]. Therefore, the coupling of graphene with the photocatalyst has offered incredible open doors for moving forward photocatalytic CO_2 decrease productivity to meet the practical requirements

Liang *et al.* observed that , coupling of graphene with semiconductor has been known as one of the most viable approache to enhance the photocatalytic CO_2 reduction activity [55]. It was found that graphene nanosheet can greatly improve the electron–hole separation rate and particular surface area of the photo catalyst. Furthermore, the coupling of graphene and semiconductor recommends the possibility of manufacturing new multicomponent composite materials that show synergistic physicochemical properties. Generally, the preference of graphene-based photocatalysts for CO_2 reduction can be arranged into 6 perspectives

(1) Suppressing photogenerated transporter recombination: Graphene has a single atom thick nanosheet of sp^2 hybridized planar structure organized in a honeycomb lattice with great conductivity, making it a great electron acceptor amid photocatalytic reaction.[56]Moreover, given the Fermi level of graphene (0 V versus NHE) is lower than the conduction band of most photocatalysts, a quick electron exchange from photocatalyst to graphene can be accomplished on graphene-based photocatalysts as a result of the band alignments. Hence, under light irradiation, the photoinduced electrons on photocatalyst can be transferred to the graphene quickly for reduction process; then, photoinduced holes can be stayed on photocatalyst for oxidation process, subsequently bringing about a high spatial separation of the photoinduced electron–hole pairs. Moreover, the electron density on the graphene nanosheet can be additionally improved, which favors multi-electron responses for photocatalytic CO_2 reduction.

(2) Enhancing specific surface area: The specific surface area of graphene is generally acknowledged as the most noteworthy among all the investigated materials due to its one atomic thick structure. Given this noteworthy specific surface area, the coupling of graphene with photocatalyst can essentially expand the specific surface area of the photocatalyst. The upgraded specific surface area can expand the surface active site on sample which is gainful for improving photocatalytic CO_2 reduction activity.

(3) Increasing CO_2 adsorption and activation: Graphene illustrates a large 2D π-conjugated structure. In meantime, CO_2 particles also contain delocalized π-conjugated restricting π[13, 57]. Hence, π–π conjugation association can be set up amongst graphene and CO_2. This remarkable π–π conjugation collaboration can altogether enhance the adsorption of CO_2 particles on the graphene-based photocatalysts, thereby improving the photocatalytic CO_2 reduction efficiency. particularly, this strong π–π conjugation cooperation amongst graphene and CO_2 can also cause destabilization and activation of CO_2 molecules, along these lines prompting a less demanding decrease of CO_2 amid the photocatalytic CO_2 reaction reaction.[58]

(4) Enhancing photostability: Given its phenomenal mechanical and chemical stability, graphene nanosheets have been appeared as compelling supporting materials in photocatalysis for improving the photostability of the photocatalyst. [58, 59]Particularly, graphene can cover on the target photocatalysts with low photostability. The graphene-based photocatalysts have great stability for long period photocatalytic CO_2 reduction application.

(5) Improving nanoparticles (NPs) scattering and reducing NPs size: Graphene arranged by synthetic strategy consist of great volume of surface functionalities , which can work as anchoring site and permit the photocatalyst to develop on its surface. [60] Therefore, photocatalyst can be consistently deposited on the surface of graphene nanosheet, so that suppressing the aggregation and development of photocatalysts. Moreover, the graphene nanosheet can likewise work as a capping agent for NPs, in this way constraining the growth of the NPs. Consequently, the photocatalyst can be controlled into smaller sizes to acquire a higher surface area, which is useful for the photocatalytic reaction.

(6) Boosting light absorption: Graphene can absorb whole spectrum due to its dark black color and zero band gap. although such great light absorption capacity does not deliver active electrons or holes for the photocatalytic reaction, it can enhance the temperature around the photocatalyst to make local photothermal effect.[59, 61] It was demonstrated that this local photothermal impact will enhance movement of reaction and product molecules, along these lines upgrading photocatalytic CO_2 reduction effciency. [61] Moreover, the photothermal effect can also enhance the charge carrier separation by generating high energy electrons on the semiconductor. Under the light irradiation, these high energy electrons can be effectively transmitted to the graphene for photocatalytic reaction instead recombining with

the hole. Nonetheless, when the stacking amount of graphene on the photocatalyst is too high, graphene can bring about a negative impact on the photocatalytic reaction. The overloading of graphene will shield the photocatalyst and disallow the photocatalyst to absorb incident light. Therefore, the generation rate of photoinduced electron–hole sets will be decreased. Along these lines, finding the ideal loading amount of graphene on the photocatalyst is needed. There was an enormous of reports about the semiconductor-graphene nanocomposite photocatalysts for CO_2 photo reduction. Strikingly, the graphene oxide can be straightforwardly connected as a promising photocatalyst for CO_2 to CH_3OH change. The biggest conversion rate of photocatalytic CO2 to CH3OH on modified graphene oxide is 0.172 μmol $gcat^{-1}$ h^{-1} under visible light, which is 6-fold higher than that of pure TiO_2. The nanocomposites based on the less defective solvent-exfoliated graphene exhibit a significantly larger enhancement in CO_2 photoreduction, especially under visible light. The rates of CO and CH_4 formations over the $Ti_{0.91}O_2$-graphene hollow spheres were 8.91 and 1.14 μmol g^{-1} h^{-1}, respectively, which was about 5 times higher than that over the $Ti_{0.91}O_2$[55, 62, 63].

3. Coupling of Semiconductors

It is generally believed that co-catalysts extract the photogenerated charge carriers from semiconductors, provide reaction sites, lower the electrochemical overpotentials associated

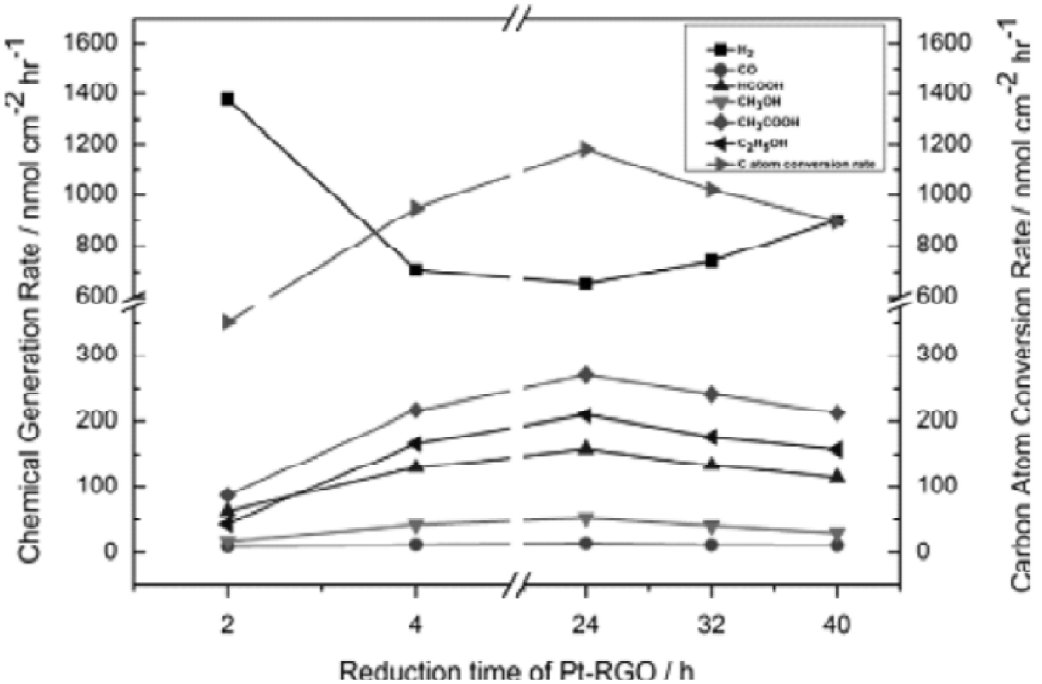

Figure 1: Carbon atom conversion rate and chemical generation rate in a photoelectrochemical cell with $PtTiO_2$ nanotube photoanode and Pt-modified reduced graphene oxide (Pt-RGO) cathode reduced for various times [69]

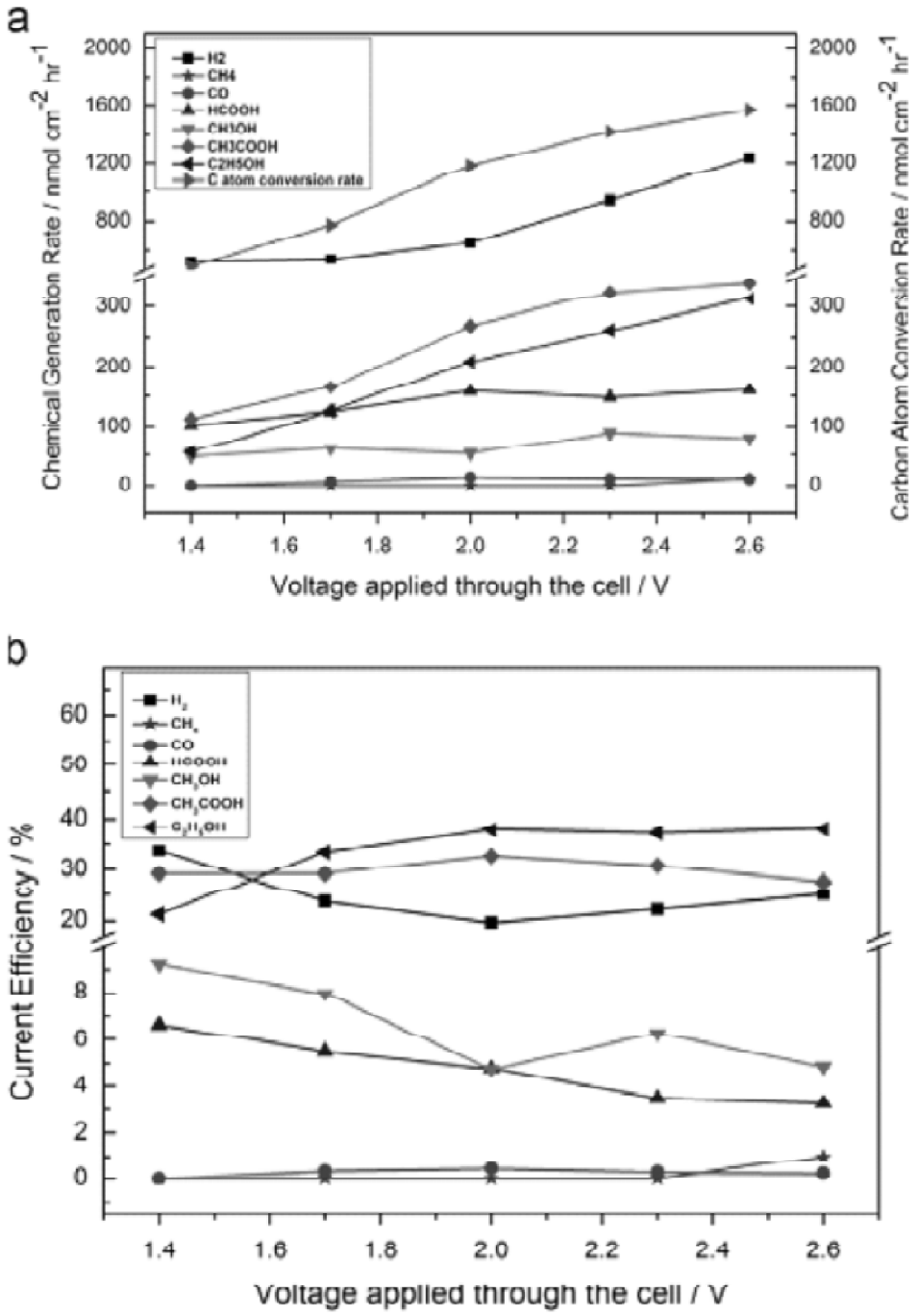

Figure 2: (a) shows the rates of CO_2 reduction product generation and C atom conversion as a function of the voltage applied through the PEC cell.methane was generated only when the potential applied was high, when the applied voltage was increased from 1.4 V to 2.6 V then the C atom conversion rate incrased form 490 nmol/(cm2 h) to 1560 nmol/(cm2 h)[69]

with the multielectron water oxidation and CO_2 reduction reactions, and decrease the activation energy for gas evolution [64, 65], it is also provide a junction/interface between the co-catalyst and the semiconductor to increase electron–hole separation/charge transport [65, 66]. In CO_2 reduction process, co-catalysts act as electron traps to increase the separation of the photogenerated electron-hole pairs and hence enhance the photocatalytic activity and selectivity for CO_2 reduction. Generally, Pd, Pt and Au can selectively reduce CO_2 into CH_4 products. shitani *et al.* [67] studied the photoreduction of CO_2 on a series of metal deposited TiO_2 and found that depositing metals (Pd, Rh, Pt, Au, Cu_2O, etc.) on TiO_2 photocatalysts can highly enhanced their photocatalytic activities for CO_2 reduction to CH_4. And additions of Pt onto the highly dispersed titanium oxide catalysts promotes the charge separation which leads to an increase in the formation of CH_4 in place of CH_3OH[68]. Jun Cheng *et al.* [69] presented that Pt-RGO||Pt-TNT photo electrochemical cell has extremely high CO_2 photo reduction efficiency with selective formation of different productions. The figure has shown the rates of CO_2 reduction production generation and C atom conversion rate of the photoelectrocatalytic process C atoms initially increased and then decreased with increasing Pt-RGO reduction time. A maximum carbon atom conversion rate of 1180 nmol/(cm2 h) was obtained when Pt-RGO was reduced for 24 h.

Fig. 2. Carbon atom conversion rate and current efficiency in a photoelectrochemical cell with Pt-TiO2 nanotubes photoanode and Pt-modified reduced grapheme oxide (PtRGO) cathode under various applied voltages: (a) C atom conversion rate and chemical generation rate, and (b) current efficiency. Note: Pt-RGO reduced for 24 h was used as cathode catalyst, and 110 PPI nickel form was used as catalyst support [69].

Recently our group used different loading ratio of graphene with PbSe/TiO_2 and observed an increase in product yield of CH_3OH. Fig. 3 (a-b) and Tables 1 and 2 show the total methanol yield and quantum yield for 48 h using a UV/visible light source. The observation of different samples clearly shows that the graphene-based ternary system highly improves the catalytic properties (Fig. 3 (c) and Table 3) and that there is a strong

Table 1
Effect of preparation method on methanol yield and quantum yield (visible light irradiation)

Sample (visible)	*CH_3OH yield ($\mu mol\ g^{-1}\ h^{-1}$)*	*Quantum yield (QE)*
PbSe-G(6%)-TiO_2 (12 h)	1.2354	0.3296
PbSe-G(6%)-TiO_2 (24 h)	2.1835	0.4165
PbSe-G(6%)-TiO_2 (36 h)	2.9778	0.5040
PbSe-G(6%)-TiO_2 (48 h)	3.3257	0.7053
Sample (visible)After Na_2SO_3	*CH_3OH yield ($\mu mol\ g^{-1}\ h^{-1}$)*	*Quantum yield (QE)*
PbSe-G(6%)-TiO_2 (12 h)	2.2574	0.3285
PbSe-G(6%)-TiO_2 (24 h)	2.9021	0.4460
PbSe-G(6%)-TiO_2 (36 h)	3.5243	0.5546
PbSe-G(6%)-TiO_2 (48 h)	3.7209	0.5979

interaction between graphene and the attached semiconductors materials. Moreover, PbSe supported by TiO_2 allows for a good interface between the PbSe and graphene nanosheet. The maximum amount of GO was found to be 6%, and this amount of graphene can provide more active sites and improve the absorption of light. But further increase in the amount of graphene beyond 6% results in a decrease in the methanol yield, as shown in Fig. 3 (d). This may be a result of an increase in the charge recombination centers or blacking out of the light[70].

Moreover the properties of TiO_2 can also be modified by attachments of metal and non-metal. A synergistic effect can be obtained with an appropriate combination of co-dopants compared to their single ion doped or undoped TiO_2 [71]. Our group also highlighted new ternary composite, Ag_2Se-G-TiO_2, using ultrasonic techniques and examined for CO_2 reduction to methanol under ultraviolet (UV) and visible light

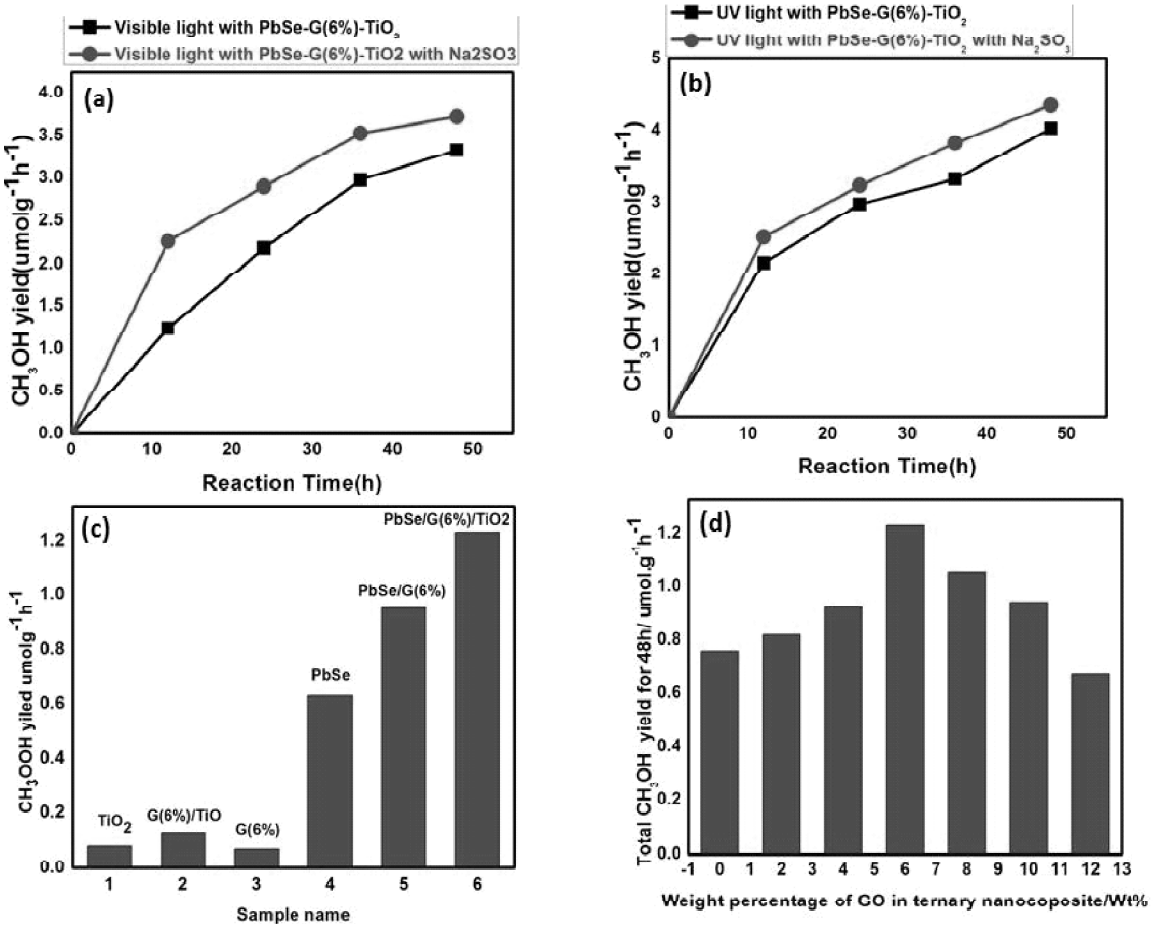

Figure 3: (a-b)The methanol yield in the photocatalytic reduction of CO_2 under UV/visible light irradiation using PbSe-G-TiO_2 nanocomposits as phtocatalysts with experimental conditions(c) The methanol yield in the photocatalytic reduction of CO_2 under UV/visible light irradiation of different nanocomposites and (d) weight percentage of grapheen in PbSe-G-TiO_2 nanocomposite [70]

Table 2
Effect of preparation method on methanol yield and quantum yield (UV light irradiation)

Sample (UV)	*CH_3OH yield ($\mu mol\ g^{-1}\ h^{-1}$)*	*Quantum yield (QE)*
PbSe-G(6%)-TiO_2 (12 h)	2.1648	0.2115
PbSe-G(6%)-TiO_2 (24 h)	2.9765	0.3806
PbSe-G(6%)-TiO_2 (36 h)	3.3252	0.4532
PbSe-G(6%)-TiO_2 (48 h)	4.0258	0.6129
Sample (UV)After Na_2SO_3	*CH_3OH yield ($\mu mol\ g^{-1}\ h^{-1}$)*	*Quantum yield (QE)*
PbSe-G(6%)-TiO_2 (12 h)	2.5149	0.3765
PbSe-G(6%)-TiO_2 (24 h)	3.2346	0.4874
PbSe-G(6%)-TiO_2 (36 h)	3.8236	0.5432
PbSe-G(6%)-TiO_2 (48 h)	4.3523	0.6345

irradiation. Ag_2Se-TiO_2 with an optimum loading graphene of 10wt% exhibited the maximum photoactivity, obtaining a total CH_3OH yield of 3.52 μmol $g^{-1}h^{-1}$ after 48h. Fig. 4(a) The photocatalytic reduction of CO_2 under UV light is more active than under visible

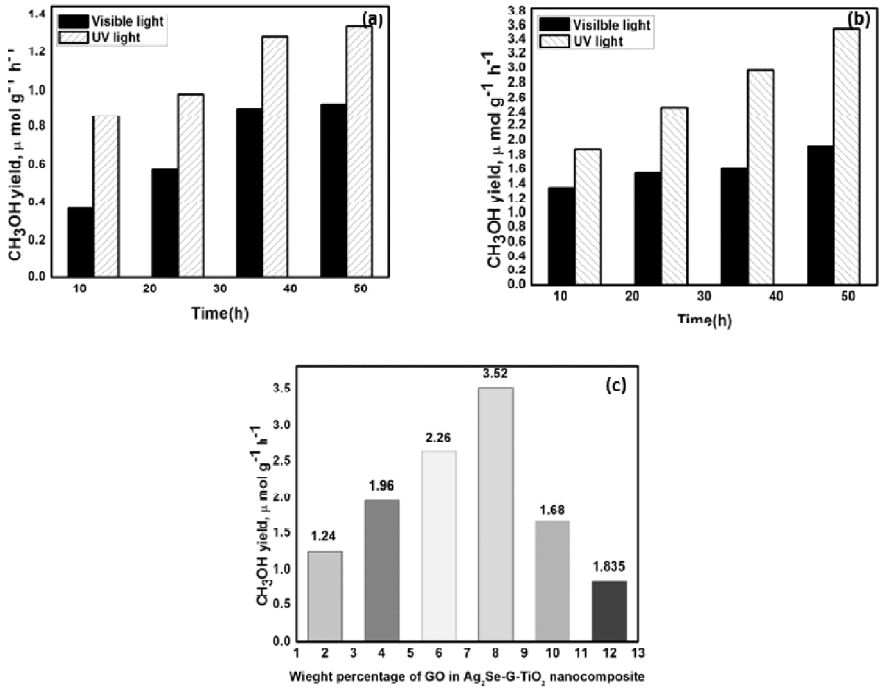

Figure 4: The methanol yield in the photocatalytic reduction of CO_2 under UV/visible light irradiation of different nanocomposites.(a) methanol yield under UV/Visible light irradiation without scavenger (b) methanol yield under UV/Visible light irradiation using Na_2SO_3 and (c) weight percentage of grapheen in Ag_2Se-G-TiO_2 nanocomposite.

light irradiation, and the maximum CH_3OH yield of Ag_2Se-G-TiO_2 after 48h was found to be 1.3420μmol g^{-1} h^{-1} without using any sacrificial reagents. Further, to improve the catalytic activity of the photoreduction of CO_2, NA_2SO_3 is used as a scavenger, as shown in Fig. 4(b). The methanol yield of Ag_2Se-G-TiO_2 under UV/Visible light is almost higher than that without using a scavenger. The CH_3OH yield of Ag_2Se-G-TiO_2 with different time intervals is shown in Table 3(a-b) and 4(a-b). The photoreduction rate of the pure TiO_2 and Ag_2Se-ghaphene nanosheets is smaller than that of the Ag_2Se-G-TiO_2 nanocomposites. This shows that a strong interaction between graphene and the attached semiconductor materials, Ag_2Se supported by TiO_2, allows good interfacial contact with the graphene sheet by enhancing the synergistic effect between Ag_2Se and the graphene sheet, which plays an important role in photoreduction activity. Hence, graphene plays an important role in the catalytic photoreduction of CO_2. The optimum content of graphene in the Ag_2Se-G-TiO_2 system was found to be 8 wt%, as shown in Fig. 4(c). The further increase in the amount of graphene in the ternary system was found to decrease the photocatalytic performance, possibly due to the increased light absorption of graphene itself, which affects the excitation of Ag_2Se and TiO_2 in the composites.

Table 3(a)
Effect of preparation method on methanol yield and quantum yield (visible light)

Sample	*CH_3OH yield ($\mu mol\ g^{-1}\ h^{-1}$)*	*Quantum yield (QE)*
Ag_2Se-G-TiO_2 (12 h)	0.3665	0.0530
Ag_2Se-G-TiO_2 (24 h)	0.5734	0.0770
Ag_2Se-G-TiO_2 (36 h)	0.9020	0.1487
Ag_2Se-G-TiO_2 (48 h)	0.9255	0.1504

Table 3(b)
Effect of preparation method on methanol yield and quantum yield (UV light)

Sample	*CH_3OH yield ($\mu mol\ g^{-1}\ h^{-1}$)*	*Quantum yield (QE)*
Ag_2Se-G-TiO_2 (12 h)	0.8623	0.1395
Ag_2Se-G-TiO_2 (24 h)	0.9814	0.1647
Ag_2Se-G-TiO_2 (36 h)	1.2821	0.2090
Ag_2Se-G-TiO_2 (48 h)	1.3420	0.1522

Table 4(a)
Effect of preparation method on methanol yield and quantum yield (visible light)

Sample After Na_2SO_3	*CH_3OH yield ($\mu mol\ g^{-1}\ h^{-1}$)*	*Quantum yield (QE)*
Ag_2Se-G-TiO_2 (12 h)	1.3380	0.2237
Ag_2Se-G-TiO_2 (24 h)	1.5450	0.2054
Ag_2Se-G-TiO_2 (36 h)	1.6100	0.2613
Ag_2Se-G-TiO_2 (48 h)	1.9170	0.3141

Table 4(b)
Effect of preparation method on methanol yield and quantum yield (UV light)

Sample After Na_2SO_3	*CH_3OH yield ($\mu mol\ g^{-1}\ h^{-1}$)*	*Quantum yield (QE)*
Ag_2Se-G-TiO_2 (12 h)	1.8862	0.3061
Ag_2Se-G-TiO_2 (24 h)	2.4682	0.4005
Ag_2Se-G-TiO_2 (36 h)	2.9683	0.4817
Ag_2Se-G-TiO_2 (48 h)	3.5262	0.5722

Also reported binary nanowire-like WSe_2-graphene nanocomposite [72]. The catalyst was prepared via ultra-sonication and was tested in terms of the photocatalytic reduction of CO_2 into CH_3OH under irradiation with UV/visible light. And photocatalytic reduction of CO_2 was tested using gas chromatography (GCMS-QP2010 SE). The methanol yields and quantum yields for the WSe_2-graphene nanocomposite with different time intervals and different conditions under UV/Visible light irradiation are shown in Tables 5 and 6. The methanol yield and quantum yield with WSe_2-graphene (12 h), WSe_2-graphene (24 h), WSe_2-graphene (36 h) and WSe_2-graphene (28 h) under visible light were 2.2434 (0.3285), 2.7021 (0.4435), 3.3243 (0.5346) and 3.5509 (0.5779) $\mu mol\ g^{-1}h^{-1}$, and under UV light were 2.8854 (0.4596), 3.1835 (0.3165), 3.7778 (0.6040) and 4.3257 (0.7053) $\mu mol\ g^{-1}h^{-1}$, respectively. And after adding Na_2SO_3 catalytic effieiceny of the binary graphene-based nanocomposites in the photoreduction of CO_2, almost two times greater than that of the nanocomposite without using scavenger (Na_2SO_3), as shown in Fig. 5(b) and Fig 5(c) shows a GC calibration curve for the quantification of methanol after 48 hours. The sacrificial reagent plays a crucial role in attaining the stability of the photocatalysts because of the well-known process of photocorrosion of sulfides. For further confirmation of final product CH_3OH, the products were recovered after 18h and 24h of irradiation and analyzed by 13C NMR (Proton decoupled) (Fig 5 d). A single peak was obtained at 48.96 ppm for both, as it is due to methanol, it is verified that photocatalytic conversions of CO_2 yield mainly CH_3OH. It is also substantiated by GC.

Table 5
Methanol Production condition with methanol yields and quantum yields under visible light

WSe_2-graphene (visible light)	*CH_3OH yields ($\mu mol\ g^{-1}\ h^{-1}$)*	*Quantum yields (QE)*
WSe_2- graphene (12 h)	2.2434	0.3285
WSe_2- graphene (24 h)	2.7021	0.4435
WSe_2- graphene (36 h)	3.3243	0.5346
WSe_2- graphene (48 h)	3.5509	0.5779
WSe_2- graphene + Na_2SO_3 (visible light)	*CH_3OH yields ($\mu mol\ g^{-1}\ h^{-1}$)*	*Quantum yields (QE)*
WSe_2- graphene (12 h)	2.8854	0.4596
WSe_2- graphene (24 h)	3.1835	0.3165
WSe_2- graphene (36 h)	3.7778	0.6040
WSe_2- graphene (48 h)	4.3257	0.7053

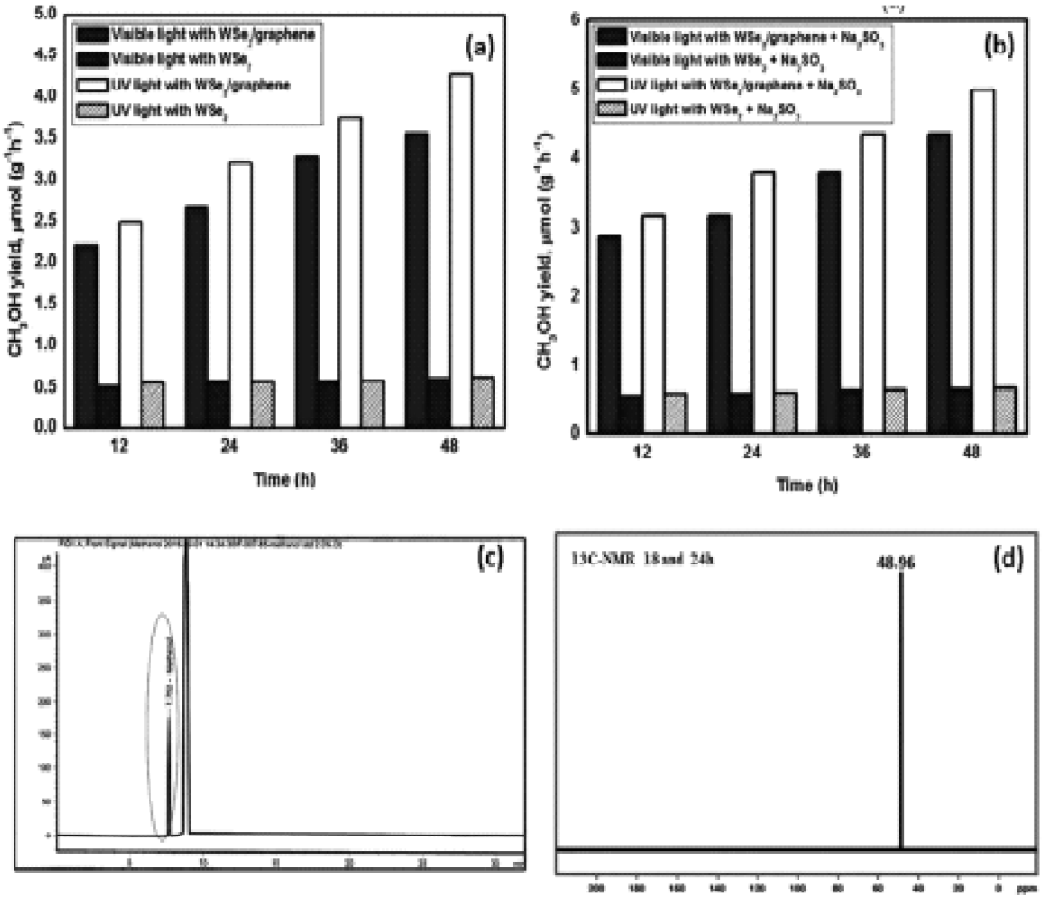

Figure 5: The methanol yields in the photocatalytic reduction of CO2 under UV/visible light irradiation by using pure WSe2 and WSe2-graphene nanocomposits as phtocatalyst (a) without Na2SO3, (b) with Na2SO3 (c) GC chromatogram of photoreaction using WSe2-graphene, after 48 h and (d) 13 C NMR (Proton decoupled) [72]

Table 6
Effect of preparation method on methanol yields and quantum yields under UV light [72]

WSe_2- graphene (UV light)	*CH_3OH yields ($\mu mol\ g^{-1}\ h^{-1}$)*	*Quantum yields (QE)*
WSe_2- graphene (12 h)	2.5134	0.3776
WSe_2- graphene (24 h)	3.2686	0.4294
WSe_2- graphene (36 h)	3.7746	0.5672
WSe_2- graphene (48 h)	2.3523	0.3535
WSe_2- graphene + Na_2SO_3 (UV light)	*CH_3OH yields ($\mu mol\ g^{-1}\ h^{-1}$)*	*Quantum yields (QE)*
WSe_2- graphene (12 h)	3.1848	0.4115
WSe_2 - graphene (24 h)	3.7765	0.5606
WSe_2- graphene (36 h)	4.3246	0.6530
WSe_2- graphene (48 h)	5.0278	0.8159

Qiuye *et al.* [73] reported a highly efficient Mgo/TiO_2 a unique one-dimensioanl (1D) nanotubes network (MgO/TNTs) films which exhibited excellent photoredution efficiency of CO_2 to methane compared with the bare TiO2 film. MgO has the strong adsorption ability of CO_2. MgO thin layer plays important role in CO_2 methantion. For the improvement of photocatalytic activity Pt nanoparticles was loaded on MgO/TNTs films. The effect of the content of MgO and MgO/TiO_2 porous films on the photoreduction performance of CO_2 was shown Fig 6. The comparison tests consisted of a reaction under light without the catalysts and in dark with catalysts. A very trace amount of CH_4 and CO was detected.

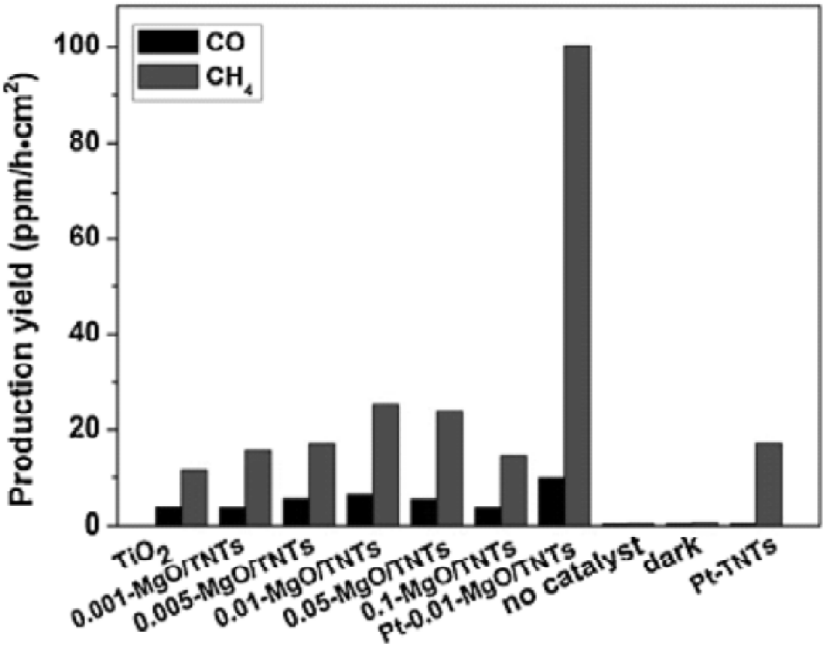

Figure 6: Photoreduction yield of CO_2 to methane and CO on the different films [73]

From the figure 5 shown there is an optimum content of MgO for CO and CH_4 formation and their generation rate firstly increased and then decreased with the increasing of MgO [73]. Byeong Sub Kwak *et al.*[74] used pure TiO_2 and Ni incorporated TiO_2 with various molar fractions using solvothermal method. The figure 6 shown that the highest amount of methane was produced when light on and after 60 min irradiation the methane yield was Ni–TiO2 (0.1 mol%) > Ni–TiO2 (0.5 mol%) > TiO_2 > Ni–TiO_2 (1.0 mol%). The best catalyst was Ni–TiO_2 (0.1 mol%) with a maximum methane yield about 14 lmol/gcatal during 60 min. and methane. However, the yield of methane was gradually decreased in repeated time.

Li *et al.* [75] used either CdS or Bi_2S_3 in the modification of the properties of TiO_2 nanotubes for CO_2 reduction under visible light irradiation. The addition of CdS or Bi_2S_3 was found to increase visible light absorbance and photocatalytic activity of TiO_2 nanotubes, with Bi_2S_3 exhibiting outstanding activity due to better surface area and CO_2

adsorption. Optimum methanol yields of 224.6 mmol/gcatal and 159.5 mmol/gcatal was observed using TiO_2 nanotubes coated with Bi_2S_3 and CdS, respectively. Heterojunction formation between the semiconductors was reported to play an important role in lengthen the lifetime of charge carriers and preventing electron/hole recombination. Although it's favorable results, this technique is not widely applied due to its drawbacks. These include photo-corrosion in aqueous phase which affects the durability and stability of the catalyst through leaching out of dopant [76, 77] and complication in finding appropriate semiconductor pairs such that recombination of charge carriers can be reduced [78].

4. Conclusion

In this review we discussed the utilization of CO_2 as a direct feedstock for photocatalytic conversion into fuels over different modification of binary and ternary Nano-composites. Application of these photocatalysis for the challenging conversion of CO_2 remains a promising pathway as it can be activated by solar energy at relatively moderate conditions to form valuable products. Although recent progress exhibited that no single material or technology meets the requirements but instead the class of technologies needs to be developed and expand to address the increasing energy use and CO_2 emission. Low selectivity and fewer availability of such materials to absorbed and reduce CO_2 is the main disadvantage in industrial application. All present technologies have their own advantages/disadvantages and restriction but their reduction/absorbance efficiency is the main difficulties. There is great need to understand the existing CO_2 reduction technologies to enhance the efficiency and fabricate cost effective catalyst materials for purification and reduction technologies.

References

[1] J. Low, B. Cheng, J. Yu, Surface modification and enhanced photocatalytic CO 2 reduction performance of TiO 2: a review, Applied Surface Science, 392 (2017) 658-686.

[2] H. Zhou, P. Li, J. Liu, Z. Chen, L. Liu, D. Dontsova, R. Yan, T. Fan, D. Zhang, J. Ye, Biomimetic polymeric semiconductor based hybrid nanosystems for artificial photosynthesis towards solar fuels generation via CO 2 reduction, Nano Energy, 25 (2016) 128-135.

[3] L.-L. Tan, W.-J. Ong, S.-P. Chai, A.R. Mohamed, Visible-light-activated oxygen-rich TiO 2 as next generation photocatalyst: Importance of annealing temperature on the photoactivity toward reduction of carbon dioxide, Chemical Engineering Journal, 283 (2016) 1254-1263.

[4] H.G. Baldoví, S.t. Neat'u, A. Khan, A.M. Asiri, S.A. Kosa, H. Garcia, Understanding the origin of the photocatalytic CO2 reduction by Au-and Cu-loaded TiO2: a microsecond transient absorption spectroscopy study, The Journal of Physical Chemistry C, 119 (2015) 6819-6827.

[5] S. Qamar, F. Lei, L. Liang, S. Gao, K. Liu, Y. Sun, W. Ni, Y. Xie, Ultrathin TiO 2 flakes optimizing solar light driven CO 2 reduction, Nano Energy, 26 (2016) 692-698.

[6] T.-m. Su, Z.-z. Qin, H.-b. Ji, Y.-x. Jiang, G. Huang, Recent advances in the photocatalytic reduction of carbon dioxide, Environmental Chemistry Letters, 14 (2016) 99-112.

[7] B. Han, W. Wei, L. Chang, P. Cheng, Y.H. Hu, Efficient visible light photocatalytic CO2 reforming of CH4, ACS Catalysis, 6 (2015) 494-497.

[8] S. Bai, W. Yin, L. Wang, Z. Li, Y. Xiong, Surface and interface design in cocatalysts for photocatalytic water splitting and CO 2 reduction, RSC Advances, 6 (2016) 57446-57463.

[9] J. Yu, J. Low, W. Xiao, P. Zhou, M. Jaroniec, Enhanced photocatalytic CO2-reduction activity of anatase TiO2 by coexposed {001} and {101} facets, Journal of the American Chemical Society, 136 (2014) 8839-8842.

[10] Y. Ma, X. Wang, Y. Jia, X. Chen, H. Han, C. Li, Titanium dioxide-based nanomaterials for photocatalytic fuel generations, Chemical reviews, 114 (2014) 9987-10043.

[11] F. Fresno, R. Portela, S. Suárez, J.M. Coronado, Photocatalytic materials: recent achievements and near future trends, Journal of Materials Chemistry A, 2 (2014) 2863-2884.

[12] I. Ganesh, Conversion of carbon dioxide into methanol–a potential liquid fuel: Fundamental challenges and opportunities (a review), Renewable and Sustainable Energy Reviews, 31 (2014) 221-257.

[13] S.N. Habisreutinger, L. Schmidt Mende, J.K. Stolarczyk, Photocatalytic reduction of CO2 on TiO2 and other semiconductors, Angewandte Chemie International Edition, 52 (2013) 7372-7408.

[14] F. Chen, Y. Li, Z. Liu, P. Fang, Facile synthesis of TiO 2/trititanate heterostructure with enhanced photoelectric efficiency for an improved photocatalysis, Applied Surface Science, 341 (2015) 55-60.

[15] L. Yuan, C. Han, M. Pagliaro, Y.-J. Xu, Origin of enhancing the photocatalytic performance of TiO2 for artificial photoreduction of CO2 through a SiO2 coating strategy, The Journal of Physical Chemistry C, 120 (2015) 265-273.

[16] P.G. Falkowski, Biotechnology and global climate change, Current Opinion in Biotechnology, 3 (1992) 286-290.

[17] M. Tahir, N.S. Amin, Recycling of carbon dioxide to renewable fuels by photocatalysis: Prospects and challenges, Renewable and Sustainable Energy Reviews, 25 (2013) 560-579.

[18] K. Li, X. An, K.H. Park, M. Khraisheh, J. Tang, A critical review of CO 2 photoconversion: catalysts and reactors, Catalysis Today, 224 (2014) 3-12.

[19] S. Solomon, G.-K. Plattner, R. Knutti, P. Friedlingstein, Irreversible climate change due to carbon dioxide emissions, Proceedings of the national academy of sciences, (2009) pnas. 0812721106.

[20] M. Tahir, N.S. Amin, Advances in visible light responsive titanium oxide-based photocatalysts for CO 2 conversion to hydrocarbon fuels, Energy Conversion and Management, 76 (2013) 194-214.

[21] D. Gust, T.A. Moore, A.L. Moore, Mimicking photosynthetic solar energy transduction, Accounts of Chemical Research, 34 (2001) 40-48.

[22] Y. Izumi, Recent advances in the photocatalytic conversion of carbon dioxide to fuels with water and/or hydrogen using solar energy and beyond, Coordination Chemistry Reviews, 257 (2013) 171-186.

[23] S. Ye, R. Wang, M.-Z. Wu, Y.-P. Yuan, A review on gC 3 N 4 for photocatalytic water splitting and CO 2 reduction, Applied Surface Science, 358 (2015) 15-27.

[24] J. Wang, C. Huang, X. Chen, H. Zhang, Z. Li, Z. Zou, Photocatalytic CO 2 reduction of BaCeO 3 with 4f configuration electrons, Applied Surface Science, 358 (2015) 463-467.

[25] M. Marszewski, S. Cao, J. Yu, M. Jaroniec, Semiconductor-based photocatalytic CO 2 conversion, Materials Horizons, 2 (2015) 261-278.

[26] S. Protti, A. Albini, N. Serpone, Photocatalytic generation of solar fuels from the reduction of H2O and CO 2: a look at the patent literature, Physical Chemistry Chemical Physics, 16 (2014) 19790-19827.

[27] H. Peng, J. Lu, C. Wu, Z. Yang, H. Chen, W. Song, P. Li, H. Yin, Co-doped MoS 2 NPs with matched energy band and low overpotential high efficiently convert CO 2 to methanol, Applied Surface Science, 353 (2015) 1003-1012.

[28] E.V. Kondratenko, G. Mul, J. Baltrusaitis, G.O. Larrazábal, J. Pérez-Ramírez, Status and perspectives of CO 2 conversion into fuels and chemicals by catalytic, photocatalytic and electrocatalytic processes, Energy & environmental science, 6 (2013) 3112-3135.

[29] A. Dhakshinamoorthy, S. Navalon, A. Corma, H. Garcia, Photocatalytic CO 2 reduction by TiO 2 and related titanium containing solids, Energy & Environmental Science, 5 (2012) 9217-9233.

[30] L. Yuan, Y.-J. Xu, Photocatalytic conversion of CO 2 into value-added and renewable fuels, Applied Surface Science, 342 (2015) 154-167.

[31] W. Dai, H. Xu, J. Yu, X. Hu, X. Luo, X. Tu, L. Yang, Photocatalytic reduction of CO 2 into methanol and ethanol over conducting polymers modified Bi 2 WO 6 microspheres under visible light, Applied Surface Science, 356 (2015) 173-180.

[32] B.S. Kwak, M. Kang, Photocatalytic reduction of CO 2 with H 2 O using perovskite Ca x Ti y O 3, Applied Surface Science, 337 (2015) 138-144.

[33] S.W. Jo, B.S. Kwak, K.M. Kim, J.Y. Do, N.-K. Park, S.O. Ryu, H.-J. Ryu, J.-I. Baek, M. Kang, Effectively CO 2 photoreduction to CH 4 by the synergistic effects of Ca and Ti on Ca-loaded TiSiMCM-41 mesoporous photocatalytic systems, Applied Surface Science, 355 (2015) 891-901.

[34] T. Inoue, A. Fujishima, S. Konishi, K. Honda, Photoelectrocatalytic reduction of carbon dioxide in aqueous suspensions of semiconductor powders, Nature, 277 (1979) 637-638.

[35] Z. Chai, Q. Li, D. Xu, Photocatalytic reduction of CO 2 to CO utilizing a stable and efficient hetero–homogeneous hybrid system, RSC Advances, 4 (2014) 44991-44995.

[36] L.-L. Tan, W.-J. Ong, S.-P. Chai, A.R. Mohamed, Reduced graphene oxide-TiO2 nanocomposite as a promising visible-light-active photocatalyst for the conversion of carbon dioxide, Nanoscale research letters, 8 (2013) 465.

[37] W.-J. Ong, L.-L. Tan, S.-P. Chai, S.-T. Yong, A.R. Mohamed, Self-assembly of nitrogen-doped TiO2 with exposed {001} facets on a graphene scaffold as photo-active hybrid nanostructures for reduction of carbon dioxide to methane, Nano Research, 7 (2014) 1528-1547.

[38] N. Patel, R. Jaiswal, T. Warang, G. Scarduelli, A. Dashora, B. Ahuja, D. Kothari, A. Miotello, Efficient photocatalytic degradation of organic water pollutants using V–N-codoped TiO 2 thin films, Applied Catalysis B: Environmental, 150 (2014) 74-81.

[39] F. Dufour, S. Pigeot-Remy, O. Durupthy, S. Cassaignon, V. Ruaux, S. Torelli, L. Mariey, F. Maugé, C. Chanéac, Morphological control of TiO 2 anatase nanoparticles: what is the good surface property to obtain efficient photocatalysts?, Applied Catalysis B: Environmental, 174 (2015) 350-360.

[40] A.J. Bard, Photoelectrochemistry, Science, 207 (1980) 139-144.

[41] A. Fujishima, K. Honda, Photolysis-decomposition of water at the surface of an irradiated semiconductor, Nature, 238 (1972) 37-38.

[42] G. Liu, M. Zhang, D. Zhang, J. Zhou, F. Meng, S. Ruan, Ultrahigh responsivity UV detector based on TiO 2/Pt-doped TiO 2 multilayer nanofilms, Journal of Alloys and Compounds, 616 (2014) 155-158.

[43] S. Bouhadoun, C. Guillard, F. Dapozze, S. Singh, D. Amans, J. Bouclé, N. Herlin-Boime, One step synthesis of N-doped and Au-loaded TiO 2 nanoparticles by laser pyrolysis: application in photocatalysis, Applied Catalysis B: Environmental, 174 (2015) 367-375.

[44] R. Asahi, T. Morikawa, T. Ohwaki, K. Aoki, Y. Taga, Visible-light photocatalysis in nitrogen-doped titanium oxides, science, 293 (2001) 269-271.

[45] Y.-C. Wu, L.-S. Ju, Annealing-free synthesis of C N co-doped TiO 2 hierarchical spheres by using amine agents via microwave-assisted solvothermal method and their photocatalytic activities, Journal of Alloys and Compounds, 604 (2014) 164-170.

[46] J. Lei, Y. Chen, F. Shen, L. Wang, Y. Liu, J. Zhang, Surface modification of TiO 2 with gC 3 N 4 for enhanced UV and visible photocatalytic activity, Journal of Alloys and Compounds, 631 (2015) 328-334.

[47] M. Wang, L. Sun, Z. Lin, J. Cai, K. Xie, C. Lin, p–n Heterojunction photoelectrodes composed of Cu 2 O-loaded TiO 2 nanotube arrays with enhanced photoelectrochemical and photoelectrocatalytic activities, Energy & Environmental Science, 6 (2013) 1211-1220.

[48] X. Huang, X. Qi, F. Boey, H. Zhang, Graphene-based composites, Chemical Society Reviews, 41 (2012) 666-686.

[49] Q. Xiang, B. Cheng, J. Yu, Graphene Based Photocatalysts for Solar Fuel Generation, Angewandte Chemie International Edition, 54 (2015) 11350-11366.

[50] Q. Li, X. Li, S. Wageh, A. Al Ghamdi, J. Yu, CdS/Graphene nanocomposite photocatalysts, Advanced Energy Materials, 5 (2015).

[51] B.F. Machado, P. Serp, Graphene-based materials for catalysis, Catalysis Science & Technology, 2 (2012) 54-75.

[52] K.S. Novoselov, A.K. Geim, S.V. Morozov, D. Jiang, Y. Zhang, S.V. Dubonos, I.V. Grigorieva, A.A. Firsov, Electric field effect in atomically thin carbon films, science, 306 (2004) 666-669.

[53] Q. Xiang, J. Yu, M. Jaroniec, Graphene-based semiconductor photocatalysts, Chemical Society Reviews, 41 (2012) 782-796.

[54] Q. Xiang, J. Yu, Graphene-based photocatalysts for hydrogen generation, The journal of physical chemistry letters, 4 (2013) 753-759.

[55] Y.T. Liang, B.K. Vijayan, K.A. Gray, M.C. Hersam, Minimizing graphene defects enhances titania nanocomposite-based photocatalytic reduction of CO2 for improved solar fuel production, Nano letters, 11 (2011) 2865-2870.

[56] D. Chen, H. Zhang, Y. Liu, J. Li, Graphene and its derivatives for the development of solar cells, photoelectrochemical, and photocatalytic applications, Energy & Environmental Science, 6 (2013) 1362-1387.

[57] X. Li, J. Wen, J. Low, Y. Fang, J. Yu, Design and fabrication of semiconductor photocatalyst for photocatalytic reduction of CO2 to solar fuel, Science China Materials, 57 (2014) 70-100.

[58] Y. Tang, X. Hu, C. Liu, Perfect inhibition of CdS photocorrosion by graphene sheltering engineering on TiO 2 nanotube array for highly stable photocatalytic activity, Physical Chemistry Chemical Physics, 16 (2014) 25321-25329.

[59] J. Yu, J. Jin, B. Cheng, M. Jaroniec, A noble metal-free reduced graphene oxide–CdS nanorod composite for the enhanced visible-light photocatalytic reduction of CO 2 to solar fuel, Journal of materials chemistry A, 2 (2014) 3407-3416.

[60] I.V. Lightcap, T.H. Kosel, P.V. Kamat, Anchoring semiconductor and metal nanoparticles on a two-dimensional catalyst mat. Storing and shuttling electrons with reduced graphene oxide, Nano Letters, 10 (2010) 577-583.

[61] Z. Gan, X. Wu, M. Meng, X. Zhu, L. Yang, P.K. Chu, Photothermal contribution to enhanced photocatalytic performance of graphene-based nanocomposites, ACS nano, 8 (2014) 9304-9310.

[62] H.-C. Hsu, I. Shown, H.-Y. Wei, Y.-C. Chang, H.-Y. Du, Y.-G. Lin, C.-A. Tseng, C.-H. Wang, L.-C. Chen, Y.-C. Lin, Graphene oxide as a promising photocatalyst for CO 2 to methanol conversion, Nanoscale, 5 (2013) 262-268.

[63] W. Tu, Y. Zhou, Q. Liu, Z. Tian, J. Gao, X. Chen, H. Zhang, J. Liu, Z. Zou, Robust hollow spheres consisting of alternating titania nanosheets and graphene nanosheets with high photocatalytic activity for CO2 conversion into renewable fuels, Advanced Functional Materials, 22 (2012) 1215-1221.

[64] K. Maeda, K. Domen, Photocatalytic water splitting: recent progress and future challenges, The Journal of Physical Chemistry Letters, 1 (2010) 2655-2661.

[65] F.E. Osterloh, B.A. Parkinson, Recent developments in solar water-splitting photocatalysis, MRS bulletin, 36 (2011) 17-22.

[66] J. Yang, D. Wang, H. Han, C. Li, Roles of cocatalysts in photocatalysis and photoelectrocatalysis, Accounts of chemical research, 46 (2013) 1900-1909.

[67] O. Ishitani, C. Inoue, Y. Suzuki, T. Ibusuki, Photocatalytic reduction of carbon dioxide to methane and acetic acid by an aqueous suspension of metal-deposited TiO2, Journal of Photochemistry and Photobiology A: Chemistry, 72 (1993) 269-271.

[68] H. Yamashita, Y. Fujii, Y. Ichihashi, S.G. Zhang, K. Ikeue, D.R. Park, K. Koyano, T. Tatsumi, M. Anpo, Selective formation of CH 3 OH in the photocatalytic reduction of CO 2 with H 2 O on titanium oxides highly dispersed within zeolites and mesoporous molecular sieves, Catalysis Today, 45 (1998) 221-227.

[69] J. Cheng, M. Zhang, G. Wu, X. Wang, J. Zhou, K. Cen, Optimizing CO 2 reduction conditions to increase carbon atom conversion using a Pt-RGO|| Pt-TNT photoelectrochemical cell, Solar Energy Materials and Solar Cells, 132 (2015) 606-614.

[70] A. Ali, W.-C. Oh, A simple ultrasono-synthetic route of PbSe-graphene-TiO2 ternary composites to improve the photocatalytic reduction of CO2, Fullerenes, Nanotubes and Carbon Nanostructures, (2017).

[71] S.G. Kumar, L.G. Devi, Review on modified TiO2 photocatalysis under UV/visible light: selected results and related mechanisms on interfacial charge carrier transfer dynamics, The Journal of Physical Chemistry A, 115 (2011) 13211-13241.

[72] A. Ali, W.-C. Oh, Preparation of Nanowire like WSe 2-Graphene Nanocomposite for Photocatalytic Reduction of CO 2 into CH 3 OH with the Presence of Sacrificial Agents, Scientific Reports, 7 (2017) 1867.

[73] Q. Li, L. Zong, C. Li, J. Yang, Photocatalytic reduction of CO 2 on MgO/TiO 2 nanotube films, Applied Surface Science, 314 (2014) 458-463.

[74] B.S. Kwak, K. Vignesh, N.-K. Park, H.-J. Ryu, J.-I. Baek, M. Kang, Methane formation from photoreduction of CO 2 with water using TiO 2 including Ni ingredient, Fuel, 143 (2015) 570-576.

[75] X. Li, H. Liu, D. Luo, J. Li, Y. Huang, H. Li, Y. Fang, Y. Xu, L. Zhu, Adsorption of CO 2 on heterostructure CdS (Bi 2 S 3)/TiO 2 nanotube photocatalysts and their photocatalytic activities in the reduction of CO 2 to methanol under visible light irradiation, Chemical Engineering Journal, 180 (2012) 151-158.

[76] H. Fujii, M. Ohtaki, K. Eguchi, H. Arai, Preparation and photocatalytic activities of a semiconductor composite of CdS embedded in a TiO 2 gel as a stable oxide semiconducting matrix, Journal of Molecular Catalysis A: Chemical, 129 (1998) 61-68.

[77] H.C. Liang, X.Z. Li, J. Nowotny, Photocatalytical properties of TiO2 nanotubes, in: Solid state phenomena, Trans Tech Publ, 2010, pp. 295-328.

[78] G. Liu, L. Wang, H.G. Yang, H.-M. Cheng, G.Q.M. Lu, Titania-based photocatalysts—crystal growth, doping and heterostructuring, Journal of Materials Chemistry, 20 (2010) 831-843.